

# **Convergent evolution of cytochrome P450s underlies independent origins of keto-carotenoid pigmentation in animals**

## **Authors**

Nicky Wybouw<sup>1</sup>, Andre H. Kurlovs<sup>1,2</sup>, Robert Greenhalgh<sup>2</sup>, Astrid Bryon<sup>1</sup>, Olivia Kosterlitz<sup>2</sup>, Yuki Manabe<sup>3</sup>, Masahiro Osakabe<sup>4</sup>, John Vontas<sup>5,6</sup>, Richard M. Clark<sup>2,7</sup>, and Thomas Van Leeuwen<sup>1</sup>

<sup>1</sup> Laboratory of Agrozoology, Department of Plants and Crops, Faculty of Bioscience Engineering, Ghent University, Coupure Links 653, B-9000 Ghent, Belgium

<sup>2</sup> School of Biological Sciences, University of Utah, 257 South 1400 East, Salt Lake City, Utah 84112, USA

<sup>3</sup> Laboratory of Technology of Marine Bioproducts, Graduate School of Agriculture, Kyoto University, Kyoto 606-8502, Japan

<sup>4</sup> Laboratory of Ecological Information, Graduate School of Agriculture, Kyoto University, Kyoto 606-8502, Japan

<sup>5</sup> Institute of Molecular Biology and Biotechnology, Foundation for Research and Technology-Hellas, 73100, Heraklion, Greece

<sup>6</sup> Department of Crop Science, Pesticide Science Lab, Agricultural University of Athens, 11855, Athens, Greece

<sup>7</sup> Center for Cell and Genome Science, University of Utah, 257 South 1400 East, Salt Lake City, Utah 84112, USA

## **Authors for correspondence**

Richard M. Clark  
School of Biological Sciences  
University of Utah  
257 South 1400 East, Rm 201  
Salt Lake City, Utah, USA 84112  
Email: richard.m.clark@utah.edu

Thomas Van Leeuwen  
Laboratory of Agrozoology  
Department of Plants and Crops  
Faculty of Bioscience Engineering  
Ghent University  
Coupure Links 653, B-9000 Ghent, Belgium  
Email: thomas.vanleeuwen@ugent.be

**Abstract**

Keto-carotenoids contribute to many important traits in animals, including vision and coloration. In a great number of animal species, keto-carotenoids are endogenously produced from carotenoids by carotenoid ketolases. Despite the ubiquity and functional importance of keto-carotenoids in animals, the underlying genetic architectures of their production have remained enigmatic. The body and eye colorations of spider mites (Arthropoda: Chelicerata) are determined by  $\beta$ -carotene and keto-carotenoid derivatives. Here, we focus on a carotenoid pigment mutant of the spider mite *Tetranychus kanzawai* that, as shown by chromatography, lost the ability to produce keto-carotenoids. We employed bulked segregant analysis and linked the causal locus to a single narrow genomic interval. The causal mutation was fine-mapped to a minimal candidate region that held only one complete gene, the cytochrome P450 monooxygenase *CYP384A1*, of the CYP3 clan. Using a number of genomic approaches, we revealed that an inactivating deletion in the fourth exon of *CYP384A1* caused the aberrant pigmentation. Phylogenetic analysis indicated that *CYP384A1* is orthologous across mite species of the ancient Trombidiformes order where carotenoids typify eye and body coloration, suggesting a deeply conserved function of *CYP384A1* as a carotenoid ketolase. Previously, *CYP2J19*, a cytochrome P450 of the CYP2 clan, has been identified as a carotenoid ketolase in birds and turtles. Our study shows that selection for endogenous production of keto-carotenoids led to convergent evolution whereby cytochrome P450s were independently co-opted in vertebrate and invertebrate animal lineages.

**Keywords**

carotenoid ketolase, convergent evolution, keto-carotenoids, lemon, *CYP384A1*

**Running head**

Carotenoid ketolase in spider mites

## 1. Introduction

Carotenoids are terpenoid pigments that are responsible for many of the bright yellow, orange and red colors observed in animals. These include the colors displayed in lizard throats, avian plumage, as well as in arthropod bodies and eggs [1,2]. In addition to coloration, carotenoids also contribute to multiple other traits in animals, such as the visual system [3–8]. For instance, in birds, carotenoids are deposited in retinal oil droplets where they function as long-pass cut-off filters to enhance color discrimination [8]. Although carotenoid pigments are widespread in the natural world, their biosynthesis occurs primarily in plants, fungi, bacteria and archaea. While most animals lack the ability to biosynthesize carotenoids, many obtain, deposit, and modify the carotenoids they encounter in their diets. Animal carotenoid ketolases add a double-bonded oxygen molecule at the C4 and/or C4' position of the terminal rings of carotenoid structures, thereby converting more yellow-colored carotenoids like  $\beta$ -carotene to more orange- and red-colored keto-carotenoid derivatives [9]. The identification of the molecular mechanisms that underpin animal carotenoid metabolism are beginning to inform the evolutionary history and adaptive function of carotenoid-based traits [10]. For instance, recent work identified the cytochrome P450 *CYP2J19* as the carotenoid ketolase responsible for keto-carotenoid production in both the integument and retinal oil droplets of birds where keto-carotenoids fulfill different biological roles [11,12].

Studies on the pigmentation of spider mites (Chelicerata: Trombidiformes), started as early as 1914, revealed that the orange-red body and red eye colorations of mites within the *Tetranychus* genus depend solely on carotenoid pigments [13–18]. A largely conserved carotenoid metabolic pathway that produces red keto-carotenoids from  $\beta$ -carotene has been proposed for tetranychids (figure 1a) [13,15–18]. Here, a striking body color change to deep orange-red is associated with diapause induction in adult females, and studies show that this change is the result of differential accumulation of endogenously produced keto-carotenoids (figure 1) [15,16]. Several spontaneous pigment mutants have been discovered in tetranychid populations and their carotenoid profiles have been characterized. Due to their indistinguishable carotenoid compositions, mutant phenotypes have been given identical descriptive names in different species. Two mutant phenotypes, albino and lemon, completely lack keto-carotenoid production [4,16,17,19]. Both albino and lemon mutants lack eye pigmentation, but whereas albino mites lack body pigmentation, the bodies of lemon mites display yellow coloration that markedly intensifies in diapause (figure 1) [4].

Genomes from several arthropod lineages, including spider mites and aphids (Hexapoda: Hemiptera), harbor horizontally transferred genes of fungal origin that code for carotenoid biosynthetic enzymes [4,20,21]. The discovery of these fungal genes embedded within arthropod genomes challenged the assumption that all animals lack the ability to biosynthesize carotenoids. Recently, inactivation of one of the horizontally acquired carotenoid biosynthetic genes, a phytoene desaturase, was shown to underlie albinism in *Tetranychus urticae* [4]. This finding, along with work on aphids [21], has revealed that the horizontally transferred biosynthetic genes remained active. Further, Bryon *et al.* [4] concluded that the carotenoid metabolic pathway of spider mites relies solely (or nearly so) on endogenously produced  $\beta$ -carotene.

Despite the recent study linking phytoene desaturase activity to endogenous  $\beta$ -carotene synthesis in spider mites, it has remained elusive how the orange and red keto-carotenoids that typify the body and eye colors of spider mites and related trombidiform mites are produced. In the early 1970s, Veerman suggested that lemon mutations disrupt carotenoid ketolase activity, inhibiting the formation of the keto-carotenoid echinenone and its downstream derivatives from  $\beta$ -carotene [16,17] (figure 1a). The lemon mutants studied by Veerman and co-authors no longer exist [3,16,17]; however, we recently recovered a new lemon pigment mutant in the spider mite *Tetranychus kanzawai*. Taking advantage of the chromosome-level genome assembly of the closely related species *T. urticae* [22], we performed bulked segregant analysis (BSA) genetic mapping to identify the locus underlying the lemon phenotype. As revealed by fine-mapping, the lemon phenotype resulted from an inactivating deletion in the fourth exon of a cytochrome P450, *CYP384A1*. *CYP384A1* belongs to the CYP3 clan, and was conserved among sequenced genomes within the ancient Trombidiformes mite order. Our study shows that the rich orange and red colorations of many vertebrate and invertebrate animals have arisen by the convergent evolution of cytochrome P450s.

## 2. Materials and methods

### (a) Mite strains

The lemon mite strain, hereafter Jp-lemon, arose as a spontaneous mutant in a population of *T. kanzawai* collected from Japanese bindweed (*Calystegia japonica* Choisy) in Kyoto, Japan (hereafter Jp-WT). A second wild-type *T. kanzawai* population, hereafter Jp2-WT, was collected from Muskmelon (*Cucumis melo*) in Iwata, Japan. An inbred line from the Jp-lemon strain was generated by six sequential rounds of mother-son matings after Bryon *et al.* [4], and is hereafter referred to as Jp-inbred-lemon. Mites were reared on potted plants or detached leaves of

*Phaseolus vulgaris* L. cv 'Speedy'. Unless otherwise stated, mite cultures were maintained at 26°C, 60% RH and a 16:8 light:dark (L:D) photoperiod.

### **(b) Mode of inheritance**

The mode of inheritance of the Jp-lemon pigment phenotype was determined by performing reciprocal crosses with Jp-WT and Jp2-WT. In each cross, 20 virgin females were placed with 30 males on a detached bean leaf and allowed to mate. The pigment phenotype was scored in F1 females to identify a recessive or dominant mode of inheritance. During F1 development, 20 female teleochrysalids (nymphal females in their final quiescent stage) were selected and placed on a separate bean leaf. Upon eclosion, the unfertilized females were transferred to new detached bean leaves on a daily basis throughout their oviposition period. Due to the arrhenotokous mode of reproduction of *T. kanzawai*, F1 virgin females only produce haploid F2 males. The mutant and wild-type pigment phenotypes in the F1 and F2 generations were scored based on body and eye color in adult mites. The hypothesis of a monogenic, recessive mode of inheritance was tested with  $\chi^2$  goodness-of-fit tests in R (version 3.4.3) [23].

### **(c) TLC and HPLC analysis of carotenoid profiles**

Extraction of bean and mite carotenoid pigments for thin-layer chromatography (TLC) analysis was based on previous work [16–18]. After collection, mite and bean leaf material was immediately transferred to 10 ml and 15 ml of ice-cold acetone, respectively. Mite and bean samples were homogenized using glass pestles. After sedimentation by gravity, the supernatants were transferred twice to a new glass vial. Five ml of hexane was added and the mixture was transferred to a glass separating funnel. Carotenoids were translocated to the hexane phase by washing the hexane-acetone mixture four times with 10 ml of water. Any residual water was carefully removed from the solution using the glass separating funnel. The solution was subsequently evaporated to complete dryness under vacuum at room temperature. Carotenoids were re-suspended in 100  $\mu$ l of hexane and spotted on a HPTLC silica 60 plate (EMD Millipore). Mobile phases of 20% and 25% acetone in hexane were run to separate carotenoids with high and low retention values ( $R_f$ ), respectively.

For high-performance liquid chromatography (HPLC) analysis, we followed previous work on carotenoid characterization [15]. Non-diapausing and diapausing adult females were obtained by placing two-day-old eggs under long-day (25°C and 16:8 L:D photoperiod) and short-day (20°C and 9:15 L:D photoperiod) conditions, respectively. To identify and quantify astaxanthin and  $\beta$ -carotene, 30 females of each treatment were collected in three replicates and homogenized in 1

ml of acetone. The homogenate was filtrated using a glass syringe with a membrane possessing a pore size of 0.45  $\mu\text{m}$  (Minisart RC4 17822; Sartorius Stedim Biotech GmbH, Goettingen, Germany). The filtrate was dried under a nitrogen gas flow and dissolved in 300  $\mu\text{l}$  of methanol. Five  $\mu\text{l}$  of the solution was used for HPLC analysis (supplementary materials and methods). Carotenoids were quantified by monitoring the absorbance at 450 nm. External calibration curves were constructed with authentic standards (astaxanthin: AG Scientific, San Diego, CA;  $\beta$ -carotene: Wako Pure Chemical Industries, Osaka, Japan). Beta-carotene levels were compared by a two-way ANOVA, followed by a Tukey test in R [23].

**(d) BSA experimental set-up, genomic sequencing and variant detection**

A segregating mite population generated by crossing Jp-inbred-lemon to Jp2-WT was used to genetically map the lemon phenotype (supplementary materials and methods). Approximately 10-12 generations after the initial cross, three replicates of 1100, 900 and 500 lemon females were collected, as were 1500 phenotypically wild-type females. For these four populations and the two parents, genomic DNA was prepared (supplementary materials and methods). RNA was extracted from 110 adult females isolated from the segregating population using an RNeasy Minikit (Qiagen) per replicate. Two RNA replicates were collected for wild-type and lemon mites. Illumina libraries for the DNA and RNA samples were prepared and sequenced at the Huntsman Cancer Institute at the University of Utah to generate paired-end genomic DNA reads of 125 bp with library insert sizes of  $\sim 700$  bp, and RNA-seq reads of insert sizes of  $\sim 335$  bp. Genomic DNA reads were aligned to the three chromosomes of *T. urticae* [22] using the default settings of BWA (version 0.7.15-r1140) [24]. Alignments were sorted by position using SAMtools 1.3.1 [25]. Duplicate reads were marked using Picard Tools 2.6.0 (<https://broadinstitute.github.io/picard/>), and indel realignment was performed using GATK (version 3.6.0-g89b7209) [26] following GATK's best practices recommendations [27,28]. GATK's UnifiedGenotyper was used for joint variant calling across all samples to identify single nucleotide differences and indels. RNA-seq reads were aligned to the *T. urticae* chromosomes using default settings of STAR (version 2.5.3a) [29], and the resulting alignments were indexed by SAMtools 1.3.1 [25].

**(e) BSA genetic mapping**

Prior to BSA mapping, the 2,419,446 nucleotide variable positions predicted between the *T. kanzawai* DNA samples and the *T. urticae* reference sequence by GATK were filtered with quality control settings adapted from GATK Doc # 2806

(<https://software.broadinstitute.org/gatk/documentation/article.php?id=2806>) (supplementary materials and methods). From the resulting 1,150,705 nucleotide positions, 196,214 single nucleotide polymorphisms (SNPs) within *T. kanzawai* were identified as fixed for contrasting differences between the two parents, and were retained. The locus responsible for the lemon phenotype was identified by comparing allele frequencies between the three lemon selected samples to the wild-type sample using previously published BSA genetic mapping methods with statistical testing for genotype-phenotype associations by permutation [22]; 75 kb windows with 5 kb offsets were used with the false discovery rate (FDR) set to 5%. Genome annotation of the BSA peak was based on Wybouw *et al.* [22].

#### **(f) De novo assemblies**

DNA sequence reads were imported into CLC Genomics Workbench 9.0.1 (<https://www.qiagenbioinformatics.com/>), trimmed using default settings, assembled into contigs using the default settings of the “De Novo Assembly” tool, and the contigs were aligned to the *T. urticae* genome assembly using BLASR (version 1.3.1) [30]. *CYP384A1* transcripts were assembled into contigs using Trinity 2.5.1 [31,32] with default settings and basic trimming by Trimmomatic [33]. Open reading frames in the Trinity-assembled contigs were predicted using TransDecoder v5.0.2. (<https://github.com/TransDecoder/TransDecoder/wiki>) [32].

#### **(g) Fine-mapping the lemon locus**

A second segregating population was generated by crossing Jp-inbred-lemon to Jp2-WT (supplementary materials and methods). For genotyping, genomic fragments polymorphic between the two parents in the region of the BSA peak were PCR-amplified and sequenced using 429 phenotypically lemon and 50 wild-type single adult females from the segregating population (supplementary materials and methods).

#### **(h) CYP phylogenetic reconstruction**

All CYP3 clan members were retrieved from nine arthropod and one tardigrade species with available annotated genome assemblies, and genomes of three mite species of the Acariformes superorder were additionally screened for close homologues to *CYP384A1*. Cytochrome P450s of the CYP2 clan were selected to root the phylogenetic tree (supplementary materials and methods). After filtering (supplementary materials and methods), the sequence set was aligned using the E-INS-i strategy of MAFFT, leaving “gappy” regions, and with 1000 cycles of iterative refinement [34]. Identical amino acid sequences were removed from the final aligned



dataset, resulting in a final set of 229 CYP sequences (supplementary table 2). The LG+I+G+F model of protein evolution was used based on the corrected Akaike Information Criterion with PartitionFinderProtein (greedy search algorithm using RAxML and one datablock) [35,36]. Maximum-likelihood searches (n=20, using randomized stepwise addition parsimony trees) and bootstrapping (n=1000) were performed using RAxML (version 8.2.10) [36], with the random number seed set at 54321.

### 3. Results

#### (a) The carotenoid profile and mode of inheritance of the lemon phenotype

A spontaneous pigment mutant, Jp-lemon, arose in the *T. kanzawai* Jp-WT population. Specifically, Jp-lemon mites lacked wild-type red pigmentation in the two eye spots, body, and the distal segments of the front legs. Instead, Jp-lemon mites displayed yellow body coloration matching descriptions of the lemon phenotype, including marked intensification in diapausing females (figure 1d,e) [16,17,19,37]. Neither wild-type nor lemon females displaying diapausing coloration (figure 1c,e) laid eggs, the canonical reproductive criterion for diapause. Lemon females entered diapause at an incidence comparable to wild-type females on the same genetic background (supplementary materials and methods, supplementary table 3).

Biochemical characterization by TLC in previously identified but now extinct lemon mutants revealed the absence of endogenously produced keto-carotenoids [16,17]. Using the same approach, we compared the carotenoid pigment profiles of wild-type and lemon mites, and their diet (kidney bean), to assess the presence of mite-specific keto-carotenoids. Two mobile phases visibly separated the mite and bean carotenoid pigments on HPTLC silica plates (figure 2). As assessed in comparison to earlier TLC studies [16–18], the plant pigments  $\alpha$ -carotene, chlorophyll a, chlorophyll b, chlorophyll derivatives, lutein, lutein 5,6-epoxide, violaxanthin and neoxanthin appeared to be present in both wild-type and lemon mite extracts, consistent with the expected ingestion of plant tissue. The profile of wild-type mites revealed the presence of endogenously produced red-colored keto-carotenoids that are likely esterified *in vivo* [16–18] (figure 2, indicated by k). In contrast, TLC analysis showed that lemon mites entirely lacked these keto-carotenoids. To further examine the carotenoid content of the newly isolated lemon mutant, we quantified  $\beta$ -carotene and astaxanthin levels by absorption spectra in an HPLC system using exogenous standards (figure 3, supplementary figure 1). Beta-carotene was present in both lemon and wild-type mites, but was detected in significantly higher concentrations in the former (two-way ANOVA,  $F_{1,11}=9.748$ ,  $p=0.0142$ ) (figure 3a). While astaxanthin accumulated in both feeding



and diapausing wild-type mites, no free astaxanthin was detected in lemon mites using non-esterified astaxanthin as the exogenous standard (figure 3b).

To establish the mode of inheritance of lemon pigmentation, we performed reciprocal crosses between Jp-lemon and two wild-type populations, Jp-WT and Jp2-WT. All diploid female F1 progeny were phenotypically wild-type, and their haploid F2 sons were wild-type or lemon in phenotype in an ~1:1 ratio (table 1), establishing a monogenic, recessive genetic basis as reported previously for lemon mutants in tetranychids [19,38].

### (b) Localization of the lemon mutation

To identify the locus underlying lemon pigmentation, we crossed inbred, diploid lemon females to a single, haploid wild-type male of the non-related Jp2-WT population. After multiple generations of sib-mating, we performed high-throughput DNA sequencing of three replicates of lemon selected and one replicate of wild-type selected offspring from the resultant bulk population. Consistent with monogenic recessive inheritance, BSA genetic mapping revealed a single genomic region underlying the lemon phenotype (figure 4, supplementary figure 2). Using the wild-type selected offspring pool as reference, the average allele frequency of the three lemon selected offspring pools peaked at position 14,287,500 bp on chromosome 1 (figure 4).

The region surrounding this peak harbored a small number of genes, of which we identified the cytochrome P450 gene *CYP384A1* (*tetur38g00650* in the *T. urticae* annotation) as a likely candidate as cytochrome P450s have been implicated in keto-carotenoid production in other taxa [11,12,39–41]. To retain or exclude *CYP384A1* as the gene responsible for keto-carotenoid synthesis, we performed fine-mapping with PCR-based markers using a population that segregated for the lemon mutation for ~10-12 generations. By genotyping with a set of markers flanking the peak BSA/*CYP384A1* region, followed by iterative genotyping of informative recombinants, we established a minimal candidate region for the lemon phenotype of only 8.96 kb. This interval harbored the entire *CYP384A1* gene, as well as a 3' end fragment of a neighboring gene (*tetur38g00660* in *T. urticae*, which encodes a protein with an Immunoglobulin-like domain (IPR007110)) (figure 4b, supplementary figure 3, and supplementary table 4).

### (c) The lemon mutation and its impact on *CYP384A1*

Coverage of Illumina read alignments from the segregating populations, as well as that of the parents, to the *T. urticae* genome revealed a likely structural variant in *T. kanzawai* within the minimal candidate region that was specific to the lemon parent, and the three lemon selected populations (lack of read coverage at ~14.2788 Mb, black arrow in figure 4c). To investigate

further, we generated *de novo* assemblies of the parents and segregating populations. In assemblies of the three lemon selected populations (contigs 3098, 441 and 996 from assembly lemonBSA1, lemonBSA2 and lemonBSA3, respectively), as well as parental Jp-inbred-lemon (contig 2665), a 246 bp deletion coupled with a 7 bp insertion (sequence CCTACCT) was present as compared to the *T. urticae* reference sequence and contig 1805 from the parental Jp2-WT strain. Cloning confirmed that the indel was located within the coding sequence of *T. kanzawai* *CYP384A1*, which was intact in wild-type *T. kanzawai*. The wild-type selected population used for BSA mapping is expected to segregate for the recessive lemon mutation, and two contigs were assembled from this population, one with the deletion and one without (contigs 487 and 21233, respectively). RNA-seq alignments, as well as localized *de novo* transcriptome assemblies for *CYP384A1*, revealed that *CYP384A1* was expressed in both lemon and wild-type mites, and confirmed that the structural variant was unique to the former (supplementary figure 4). With a PCR-based marker, we also found that the deletion segregated perfectly with the lemon phenotype in the individuals used for fine-mapping (supplementary table 4). Apart from the 246/7 bp deletion/insertion, the genome and transcriptome assemblies revealed no other large structural variants, and no other fixed coding changes were found between the lemon and wild-type mites within the minimal 8.96 kb candidate region.

The 246/7 bp deletion/insertion was located internal to exon 4 of *CYP384A1*, and introduced a frameshift that results in a premature stop codon before the splice site at the 3' end of exon 4. As a result of the deletion and frameshift, only the first 384 of the 497 amino acids present in the wild-type *CYP384A1* of *T. kanzawai* are predicted to be encoded in lemon mites. The Helix K, PERF and heme binding motifs essential for CYP enzymatic activity were absent in the truncated *CYP384A1* protein (figure 4d and supplementary figure 4).

**(d) Evolutionary history of CYP384A1**

We investigated the evolutionary origin of *CYP384A1* by a maximum-likelihood phylogenetic analysis using the CYP3 clans of 12 arthropods and one tardigrade, rooted by CYPs of the CYP2 clan (a total of 229 CYPs) (figure 5 and supplementary figure 5). *CYP384A1* exhibited a clear 1:1:1:1 orthology across all analyzed mite species of the Trombidiformes order (*T. urticae*, *Panonychus ulmi*, *Dinothrombium tinctorium*, and *Leptotrombidium deliense*). Three copies were initially identified in the *D. tinctorium* genome assembly, but were finally considered as putative allelic variants (lowest degree of sequence identity was 93.62% and the scaffolds that hold the copies did not code for additional proteins). *CYP383A1*, the closest homologue to *CYP384A1* within *T. urticae* [20], also exhibited a clear 1:1:1:1 orthology across the four trombidiform mites.

The CYP383A1 and CYP384A1 groups were clustered with strong bootstrap support and this well-supported clade only included CYP sequences from trombidiform mites (supplementary figure 5).

#### 4. Discussion

As opposed to pigments like melanin, relatively little is known about the transport, modification and deposition of the diverse set of carotenoid pigments in animals [10]. Here, we identified a cytochrome P450 of the CYP3 clan, *CYP384A1*, as a likely carotenoid ketolase by showing that an inactivating deletion is strictly associated with the lemon pigment phenotype that lacks keto-carotenoids. Recent genomic research on zebra finches and canaries implicated CYP2J19, a cytochrome P450 of the CYP2 clan, as the main (or only) carotenoid ketolase enzyme in birds that produces keto-carotenoids in the integument and retinal oil droplets [11,12,42]. Although the exact enzymatic abilities of CYP2J19 and CYP384A1 remain unknown, it is very likely that these cytochrome P450s not only hydroxylate, but also oxidize carotenoid substrates at the C4 and/or C4' positions of the terminal rings. Carotenoid profiles of the spider mite *T. urticae* and the bird *Cardinalis cardinalis* have been characterized in detail and no hydroxylated intermediates were identified [16,43]. In addition, in the fungus *Xanthophyllomyces dendrorhous*, a single cytochrome P450 is able to produce keto-carotenoids from a carotenoid precursor [39,40]. Our work now provides compelling evidence that birds and spider mites have addressed the biochemical challenge of producing keto-carotenoids by independent, convergent evolution across the CYP2 and CYP3 clans. Our findings add to several other examples of convergent evolution within this diverse multi-gene family, including the biosynthesis of cyanogenic glycosides in insects and plants [44], the production of growth-regulating gibberellins in plants and fungi [45], and syringyl lignin biosynthesis in lycophytes and flowering plants [46]. CYP383A1, the closest homologue to CYP384A1 in the *T. urticae* genome, is a potential candidate for an additional ketolase in spider mites, one that could potentially produce more oxygenated keto-carotenoids, such as astaxanthin, in which keto- and hydroxyl groups are present on both terminal cyclic rings of the  $\beta$ -carotene precursor backbone. It is also possible that CYP384A1, as well as CYP2J19, are multifunctional and able to produce different keto-carotenoids by multistep conversion, as observed in *X. dendrorhous*, where a single cytochrome P450 is strongly implicated in the conversion of  $\beta$ -carotene to astaxanthin [39,40].

Phylogenetic analysis suggests that *CYP2J19* arose via gene duplication prior to the turtle-archosaur split and that a homologue has been maintained in turtles but lost in crocodiles [41]. It is also suggested that *CYP2J19* originally played a role in color vision by producing keto-

carotenoids in retinal oil droplets and was independently co-opted in certain bird and turtle lineages for a role in integument coloration-based signaling [41,42]. Our phylogenetic reconstruction uncovered that *CYP384A1*, *CYP383A1*, and their orthologues are restricted to mites within the speciose Trombidiformes order, an ancient lineage that originated about 400 MYA [47,48]. Consistent with our hypothesis that the orthologous group containing *CYP384A1* has a conserved carotenoid ketolase function, this order holds a high number of species that accumulate  $\beta$ -carotene and keto-carotenoid derivatives [49,50]. In contrast to the great majority of animals, including birds, previous work has strongly indicated that spider mites are able to biosynthesize  $\beta$ -carotene due to the lateral acquisition of fungal carotenoid biosynthetic genes and no longer depend on dietary salvage [4,51]. Interestingly, the horizontal transfer of carotenoid biosynthetic genes into mites occurred early in the evolution of the Trombidiformes order [51]. This raises the question of whether these cytochrome P450 enzymes were co-opted for keto-carotenoid production following the lateral acquisition. Although speculative, the horizontal transfer of carotenoid biosynthetic genes and the early evolution of *CYP384A1* may have facilitated the appropriation of keto-carotenoids as the dominant pigments in many trombidiform mites.

Body coloration is known to have many adaptive functions in animals, including sexual, social, and interspecific signaling [2,52]. Using water mites and fish predators as a biological system, Kerfoot [53] reasoned that the red-colored, carotenoid-based body coloration serves an aposematic function in trombidiform mites, but more recent studies on the same system have reported contradictory results [54,55]. Carotenoid pigments have been implicated in protection against oxidative stress in various other animals [56], and currently the most popular hypothesis is that the keto-carotenoid accumulation in mite bodies is protective against light-associated oxidative damage in Trombidiformes. In support, Atarashi *et al.* [13] showed that albino *Panonychus citri* mites have a decreased non-enzymatic antioxidant capacity compared to wild-type mites. In addition, relative to non-diapausing *T. urticae*, diapausing *T. urticae* mites, which accumulate higher levels of keto-carotenoids [15,16], exhibit a higher resistance to UV light that induces reactive oxygen species [57]. Together, these studies suggest that carotenoids facilitate spider mite survival during long periods of increased UV exposure, although protection against other inducers of oxidative stress cannot be ruled out. Carotenoid metabolism is also critical for the animal visual system [10]. Visual chromophores, which function in phototransduction, rely on the enzymatic cleavage and modification of carotenoids into apo-carotenoids (vitamin A precursors) and disruption of these carotenoid metabolic pathways impairs vision [6,7]. In *T. urticae*, one of the horizontally acquired genes that allow for  $\beta$ -carotene biosynthesis is essential

for diapause induction, reflecting the requirement of  $\beta$ -carotene as a precursory compound to perceive the inductive photoperiods [4]. We found that lemon *T. kanzawai* did not exhibit a decreased diapause incidence compared to its wild-type genetic background, supporting the hypothesis that light perception in spider mites depends on  $\beta$ -carotene but not its keto-carotenoid derivatives [3,4,37]. Biochemical and genetic work on previously recovered carotenoid pigment mutants strongly indicates that the spider mite eye spots owe their bright red coloration to an accumulation of esterified astaxanthin [16,17]. Astaxanthin might therefore act as a light filter, possibly protecting underlying photoreceptors from damage by intense light, a role also performed by the chemically unrelated ommochrome and pteridine pigments in the compound eyes of insects like *Drosophila melanogaster* [58,59]. Our findings shed light on the evolutionary history of keto-carotenoid production in trombidiform mites and open up new avenues to understand the potential adaptive value of keto-carotenoid-based traits in these invertebrates.

## Funding

This project has received funding from the European Research Council (ERC) under the Horizon 2020 research and innovation program, grant agreement No 772026–POLYADAPT (to T.V.L.) and No 773902–SUPERPEST (to T.V.L.) and by the USA National Science Foundation (award 1457346 to R.M.C.). N.W. was supported by a Research Foundation - Flanders (FWO) fellowship (12T9818N). R.G. was funded in part by the National Institutes of Health Genetics Training Grant T32GM007464. The content is solely the responsibility of the authors and does not necessarily represent the official views of the funding agencies.

## Acknowledgements

We thank Xiaofeng Dong, Alistair Darby, and Benjamin Makepeace for sharing the *L. deliense* and *D. tinctorium* proteomes ahead of peer-reviewed publication. We thank René Feyereisen for insightful discussions on cytochrome P450 function and phylogeny and Jan van Arkel for technical assistance in photography. We are indebted to Tomoe Sekido and Tatsuya Sugawara for their help with the HPLC experiments. Sequencing data for this study was generated by the Genomics Core Facility of the Health Sciences Cores at the University of Utah.

**Table 1. Lemon pigmentation has a recessive, monogenic mode of inheritance in *T. kanzawai***

Cross (♀ x ♂)	% lemon in F1 ♀ (2n)	F2 ♂ (n)		$\chi^2$	p-value
		wild-type	lemon		
Jp-WT x Jp-lemon	0	175	196	1.1887	0.2756
Jp-lemon x Jp-WT	0	365	372	0.066486	0.7965
Jp2-WT x Jp-lemon	0	198	210	0.35294	0.5525
Jp-lemon x Jp2-WT	0	187	174	0.46814	0.4938

The degrees of freedom for the  $\chi^2$ -tests were 1. For every cross, at least 70 F1 females were scored.



## References

1. Goodwin TW. 1984 *The Biochemistry of the Carotenoids. Volume II Animals*. London: Chapman and Hall.
2. Hill GE, McGraw KJ. 2006 *Bird coloration. Vol. 2. Function and evolution*. Cambridge: Harvard University Press.
3. Bosse ThC, Veerman A. 1996 Involvement of vitamin A in the photoperiodic induction of diapause in the spider mite *Tetranychus urticae* is demonstrated by rearing an albino mutant on a semi-synthetic diet with and without p-carotene or vitamin A. *Physiol. Entomol.* **21**, 188–192. (doi:10.1111/j.1365-3032.1996.tb00854.x)
4. Bryon A *et al.* 2017 Disruption of a horizontally transferred phytoene desaturase abolishes carotenoid accumulation and diapause in *Tetranychus urticae*. *Proc. Natl. Acad. Sci.* **114**, E5871–E5880. (doi:10.1073/pnas.1706865114)
5. Heath JJ, Cipollini DF, Stireman III JO. 2013 The role of carotenoids and their derivatives in mediating interactions between insects and their environment. *Arthropod-Plant Interact.* **7**, 1–20. (doi:10.1007/s11829-012-9239-7)
6. von Lintig J. 2010 Colors with functions: elucidating the biochemical and molecular basis of carotenoid metabolism. *Annu. Rev. Nutr.* **30**, 35–56. (doi:10.1146/annurev-nutr-080508-141027)
7. von Lintig J, Dreher A, Kiefer C, Wernet MF, Vogt K. 2001 Analysis of the blind *Drosophila* mutant *ninaB* identifies the gene encoding the key enzyme for vitamin A formation *in vivo*. *Proc. Natl. Acad. Sci.* **98**, 1130–1135. (doi:10.1073/pnas.98.3.1130)
8. Toomey MB, Collins AM, Frederiksen R, Cornwall MC, Timlin JA, Corbo JC. 2015 A complex carotenoid palette tunes avian colour vision. *J. R. Soc. Interface* **12**, 20150563. (doi:10.1098/rsif.2015.0563)
9. Britton G. 1995 Structure and properties of carotenoids in relation to function. *FASEB J.* **9**, 1551–1558.
10. Toews DPL, Hofmeister NR, Taylor SA. 2017 The evolution and genetics of carotenoid processing in animals. *Trends Genet.* **33**, 171–182. (doi:10.1016/j.tig.2017.01.002)
11. Lopes RJ *et al.* 2016 Genetic basis for red coloration in birds. *Curr. Biol.* **26**, 1427–1434. (doi:10.1016/j.cub.2016.03.076)
12. Mundy NI *et al.* 2016 Red carotenoid coloration in the zebra finch is controlled by a cytochrome P450 gene cluster. *Curr. Biol.* **26**, 1435–1440. (doi:10.1016/j.cub.2016.04.047)
13. Atarashi M, Manabe Y, Kishimoto H, Sugawara T, Osakabe M. 2017 Antioxidant Protection by Astaxanthin in the Citrus Red Mite (Acari: Tetranychidae). *Environ. Entomol.* **46**, 1143–1150. (doi:10.1093/ee/nvx121)
14. Ewing HE. 1914 The Common Red Spider or Spider Mite. *Or. Agric. Coll. Exp. Stn.* **121**.

- 485 15. Kawaguchi S, Manabe Y, Sugawara T, Osakabe M. 2016 Imaginal feeding for progression  
486 of diapause phenotype in the two-spotted spider mite (Acari: Tetranychidae). *Environ.*  
487 *Entomol.* **45**, 1568–1573. (doi:10.1093/ee/nvw127)
- 488 16. Veerman A. 1974 Carotenoid metabolism in *Tetranychus urticae* Koch (Acari:  
489 Tetranychidae). *Comp. Biochem. Physiol. Part B Comp. Biochem.* **47**, 101–116.  
490 (doi:10.1016/0305-0491(74)90095-9)
- 491 17. Veerman A. 1972 Carotenoids of wild-type and mutant strains of *Tetranychus pacificus*  
492 McGregor (Acari: Tetranychidae). *Comp. Biochem. Physiol. Part B Comp. Biochem.* **42**,  
493 329–340. (doi:10.1016/0305-0491(72)90277-5)
- 494 18. Veerman A. 1970 The pigments of *Tetranychus cinnabarinus* boisd. (Acari: Tetranychidae).  
495 *Comp. Biochem. Physiol.* **36**, 749–763. (doi:10.1016/0010-406X(70)90530-X)
- 496 19. Helle W, van Zon AQ. 1967 Rates of spontaneous mutation in certain genes of an  
497 arrhenotokous mite, *Tetranychus pacificus*. *Entomol. Exp. Appl.* **10**, 189–193.  
498 (doi:10.1111/j.1570-7458.1967.tb00058.x)
- 499 20. Grbić M *et al.* 2011 The genome of *Tetranychus urticae* reveals herbivorous pest  
500 adaptations. *Nature* **479**, 487–492. (doi:10.1038/nature10640)
- 501 21. Moran NA, Jarvik T. 2010 Lateral transfer of genes from fungi underlies carotenoid  
502 production in aphids. *Science* **328**, 624–627. (doi:10.1126/science.1187113)
- 503 22. Wybouw N *et al.* 2019 Long-Term Population Studies Uncover the Genome Structure and  
504 Genetic Basis of Xenobiotic and Host Plant Adaptation in the Herbivore *Tetranychus*  
505 *urticae*. *Genetics* , genetics.301803.2018. (doi:10.1534/genetics.118.301803)
- 506 23. R Core Team. 2017 R: A language and environment for statistical computing. R Foundation  
507 for Statistical Computing, Vienna, Austria. URL <http://www.R-project.org>.
- 508 24. Li H, Durbin R. 2009 Fast and accurate short read alignment with Burrows-Wheeler  
509 transform. *Bioinformatics* **25**, 1754–1760. (doi:10.1093/bioinformatics/btp324)
- 510 25. Li H *et al.* 2009 The Sequence Alignment/Map format and SAMtools. *Bioinformatics* **25**,  
511 2078–2079. (doi:10.1093/bioinformatics/btp352)
- 512 26. McKenna A *et al.* 2010 The Genome Analysis Toolkit: A MapReduce framework for  
513 analyzing next-generation DNA sequencing data. *Genome Res.* **20**, 1297–1303.  
514 (doi:10.1101/gr.107524.110)
- 515 27. DePristo MA *et al.* 2011 A framework for variation discovery and genotyping using next-  
516 generation DNA sequencing data. *Nat. Genet.* **43**, 491–498. (doi:10.1038/ng.806)
- 517 28. Van der Auwera GA *et al.* 2013 From FastQ data to high-confidence variant calls: The  
518 Genome Analysis Toolkit best practices pipeline. In *Current Protocols in Bioinformatics* (eds  
519 A Bateman, WR Pearson, LD Stein, GD Stormo, JR Yates), pp. 11.10.1-11.10.33. Hoboken,  
520 NJ, USA: John Wiley & Sons, Inc. (doi:10.1002/0471250953.bi1110s43)

- 521 29. Dobin A, Davis CA, Schlesinger F, Drenkow J, Zaleski C, Jha S, Batut P, Chaisson M,  
522 Gingeras TR. 2013 STAR: ultrafast universal RNA-seq aligner. *Bioinformatics* **29**, 15–21.  
523 (doi:10.1093/bioinformatics/bts635)
- 524 30. Chaisson MJ, Tesler G. 2012 Mapping single molecule sequencing reads using basic local  
525 alignment with successive refinement (BLASR): application and theory. *BMC Bioinformatics*  
526 **13**, 238. (doi:10.1186/1471-2105-13-238)
- 527 31. Grabherr MG *et al.* 2011 Full-length transcriptome assembly from RNA-Seq data without a  
528 reference genome. *Nat. Biotechnol.* **29**, 644–652. (doi:10.1038/nbt.1883)
- 529 32. Haas BJ *et al.* 2013 *De novo* transcript sequence reconstruction from RNA-seq using the  
530 Trinity platform for reference generation and analysis. *Nat. Protoc.* **8**, 1494–1512.  
531 (doi:10.1038/nprot.2013.084)
- 532 33. Bolger AM, Lohse M, Usadel B. 2014 Trimmomatic: a flexible trimmer for Illumina sequence  
533 data. *Bioinformatics* **30**, 2114–2120. (doi:10.1093/bioinformatics/btu170)
- 534 34. Katoh K, Toh H. 2010 Parallelization of the MAFFT multiple sequence alignment program.  
535 *Bioinformatics* **26**, 1899–1900. (doi:10.1093/bioinformatics/btq224)
- 536 35. Lanfear R, Frandsen PB, Wright AM, Senfeld T, Calcott B. 2016 PartitionFinder 2: New  
537 Methods for Selecting Partitioned Models of Evolution for Molecular and Morphological  
538 Phylogenetic Analyses. *Mol. Biol. Evol.* , msw260. (doi:10.1093/molbev/msw260)
- 539 36. Stamatakis A. 2014 RAxML version 8: a tool for phylogenetic analysis and post-analysis of  
540 large phylogenies. *Bioinformatics* **30**, 1312–1313. (doi:10.1093/bioinformatics/btu033)
- 541 37. Veerman A. 1980 Functional involvement of carotenoids in photoperiodic induction of  
542 diapause in the spider mite, *Tetranychus urticae*. *Physiol. Entomol.* **5**, 291–300.  
543 (doi:10.1111/j.1365-3032.1980.tb00237.x)
- 544 38. Helle W, van Zon AQ. 1970 Linkage studies in the pacific spider mite *Tetranychus pacificus*  
545 ii. Genes for white eye II, lemon and flamingo. *Entomol. Exp. Appl.* **13**, 300–306.  
546 (doi:10.1111/j.1570-7458.1970.tb00114.x)
- 547 39. Álvarez V, Rodríguez-Sáiz M, de la Fuente JL, Gudiña EJ, Godio RP, Martín JF, Barredo  
548 JL. 2006 The crtS gene of *Xanthophyllomyces dendrorhous* encodes a novel cytochrome-  
549 P450 hydroxylase involved in the conversion of  $\beta$ -carotene into astaxanthin and other  
550 xanthophylls. *Fungal Genet. Biol.* **43**, 261–272. (doi:10.1016/j.fgb.2005.12.004)
- 551 40. Ojima K, Breitenbach J, Visser H, Setoguchi Y, Tabata K, Hoshino T, van den Berg J,  
552 Sandmann G. 2006 Cloning of the astaxanthin synthase gene from *Xanthophyllomyces*  
553 *dendrorhous* (*Phaffia rhodozyma*) and its assignment as a  $\beta$ -carotene 3-hydroxylase/4-  
554 ketolase. *Mol. Genet. Genomics* **275**, 148–158. (doi:10.1007/s00438-005-0072-x)
- 555 41. Twyman H, Valenzuela N, Liteman R, Andersson S, Mundy NI. 2016 Seeing red to being  
556 red: conserved genetic mechanism for red cone oil droplets and co-option for red coloration  
557 in birds and turtles. *Proc. R. Soc. B Biol. Sci.* **283**, 20161208. (doi:10.1098/rspb.2016.1208)

- 558 42. Twyman H, Prager M, Mundy NI, Andersson S. 2018 Expression of a carotenoid-modifying  
559 gene and evolution of red coloration in weaverbirds (Ploceidae). *Mol. Ecol.*  
560 (doi:10.1111/mec.14451)
- 561 43. McGraw KJ, Hill GE, Stradi R, Parker RS. 2001 The Influence of Carotenoid Acquisition and  
562 Utilization on the Maintenance of Species-Typical Plumage Pigmentation in Male American  
563 Goldfinches (*Carduelis tristis*) and Northern Cardinals (*Cardinalis cardinalis*). *Physiol.*  
564 *Biochem. Zool.* **74**, 843–852. (doi:10.1086/323797)
- 565 44. Jensen NB, Zagrobelny M, Hjernø K, Olsen CE, Houghton-Larsen J, Borch J, Møller BL,  
566 Bak S. 2011 Convergent evolution in biosynthesis of cyanogenic defence compounds in  
567 plants and insects. *Nat. Commun.* **2**. (doi:10.1038/ncomms1271)
- 568 45. Hedden P, Phillips AL, Rojas MC, Carrera E, Tudzynski B. 2001 Gibberellin Biosynthesis in  
569 Plants and Fungi: A Case of Convergent Evolution? *J. Plant Growth Regul.* **20**, 319–331.  
570 (doi:10.1007/s003440010037)
- 571 46. Weng J-K, Akiyama T, Bonawitz ND, Li X, Ralph J, Chapple C. 2010 Convergent Evolution  
572 of Syringyl Lignin Biosynthesis via Distinct Pathways in the Lycophyte *Selaginella* and  
573 Flowering Plants. *Plant Cell* **22**, 1033–1045. (doi:10.1105/tpc.109.073528)
- 574 47. Dabert M, Witalinski W, Kazmierski A, Olszanowski Z, Dabert J. 2010 Molecular phylogeny  
575 of acariform mites (Acari, Arachnida): Strong conflict between phylogenetic signal and long-  
576 branch attraction artifacts. *Mol. Phylogenet. Evol.* **56**, 222–241.  
577 (doi:10.1016/j.ympev.2009.12.020)
- 578 48. Xue X-F, Dong Y, Deng W, Hong X-Y, Shao R. 2017 The phylogenetic position of  
579 eriophyoid mites (superfamily Eriophyoidea) in Acariformes inferred from the sequences of  
580 mitochondrial genomes and nuclear small subunit ( 18S ) rRNA gene. *Mol. Phylogenet.*  
581 *Evol.* **109**, 271–282. (doi:10.1016/j.ympev.2017.01.009)
- 582 49. Czeuczuga, Czerpak R. 1968 Pigments occurring in *Hydrachna geografica* and *Piona nodata*  
583 (Hydracarina, Arachnoidea). *Experientia* **24**, 218–219. (doi:10.1007/BF02152777)
- 584 50. Green J. 1964 Pigments of the hydracarine *Eylais extendens* (Acari: Hydrachnellae). *Comp.*  
585 *Biochem. Physiol.* **13**, 469–472. (doi:10.1016/0010-406X(64)90039-8)
- 586 51. Dong X *et al.* 2018 Genomes of trombidid mites reveal novel predicted allergens and  
587 laterally-transferred genes associated with secondary metabolism. *GigaScience*  
588 (doi:10.1093/gigascience/giy127)
- 589 52. Svensson, Wong. 2011 Carotenoid-based signals in behavioural ecology: a review.  
590 *Behaviour* **148**, 131–189. (doi:10.1163/000579510X548673)
- 591 53. Kerfoot WC. 1981 A Question of Taste: Crypsis and Warning Coloration in Freshwater  
592 Zooplankton Communities. *Ecology* **63**, 538–554. (doi:10.2307/1938969)
- 593 54. Proctor HC, Garga N. 2004 Red, distasteful water mites: did fish make them that way? In  
594 *Aquatic Mites from Genes to Communities* (ed HC Proctor), pp. 127–147. Dordrecht:  
595 Springer Netherlands. (doi:10.1007/978-94-017-0429-8\_10)

55. Walter DE, Proctor HC. 2013 Acari Underwater, or, Why Did Mites Take the Plunge? In *Mites: Ecology, Evolution & Behaviour*, pp. 229–280. Dordrecht: Springer Netherlands. (doi:10.1007/978-94-007-7164-2\_7)
56. Esteban R, Moran JF, Becerril JM, García-Plazaola JI. 2015 Versatility of carotenoids: An integrated view on diversity, evolution, functional roles and environmental interactions. *Environ. Exp. Bot.* **119**, 63–75. (doi:10.1016/j.envexpbot.2015.04.009)
57. Suzuki T, Watanabe M, Takeda M. 2009 UV tolerance in the two-spotted spider mite, *Tetranychus urticae*. *J. Insect Physiol.* **55**, 649–654. (doi:10.1016/j.jinsphys.2009.04.005)
58. Cosens D, Briscoe D. 1972 A switch phenomenon in the compound eye of the white-eyed mutant of *Drosophila melanogaster*. *J. Insect Physiol.* **18**, 627–632. (doi:10.1016/0022-1910(72)90190-4)
59. Summers KM, Howells AJ, Pylotis NA. 1982 Biology of Eye Pigmentation in Insects. In *Advances in Insect Physiology*, pp. 119–166. Elsevier. (doi:10.1016/S0065-2806(08)60153-8)
60. Dunlop JA, Alberti G. 2007 The affinities of mites and ticks: a review. *J. Zool. Syst. Evol. Res.* **46**, 1–18. (doi:10.1111/j.1439-0469.2007.00429.x)

## Figure legends

**Figure 1. The conserved keto-carotenoid biosynthesis pathway in tetranychid mites and its disruption in lemon mutants.** (a) The proposed pathway for carotenoid biosynthesis in spider mites [18] adapted to incorporate recent findings (endogenous synthesis of  $\beta$ -carotene by phytoene desaturase [4]).  $\beta$ -carotene is converted to echinenone, which leads to three major keto-carotenoids: 3-hydroxyechinenone and phoenicoxanthin (not shown), and astaxanthin [18]. Carotenoids are depicted in their de-esterified forms. (b) Wild-type *T. kanzawai*. (c) Wild-type diapausing *T. kanzawai*. (d) Lemon *T. kanzawai*. (e) Lemon diapausing *T. kanzawai*. Each panel depicts an adult female. Arrows highlight the anterior and posterior eye spots, which are red-colored in wild-type individuals. The dark regions in feeding, non-diapausing mites are gut contents that are visible through the partially translucent cuticle. Feeding spots are absent (or nearly so) in diapausing mites that have ceased to actively feed. Scalebars represent 0.1 mm.

**Figure 2. Lemon *T. kanzawai* lacks endogenously produced keto-carotenoids.** (a) and (b) show HPTLC plates for plant and mite extracts run with mobile phases of 20% and 25% acetone in hexane, respectively. Using previously determined  $R_f$  values and color profiles [16–18], we tentatively identified the carotenoid pigments as: **1**:  $\alpha$ - and  $\beta$ -carotene, **k**: keto-carotenoid (esterified *in vivo*), **2**:  $\beta$ -carotene-diepoxyde, **3**: unknown epoxide, **4**: chlorophyll a, **5**: chlorophyll b, **c**: chlorophyll derivatives, **6**: lutein and lutein 5,6-epoxide, **7**: violaxanthin, and **8**: neoxanthin.

**Figure 3. Lemon *T. kanzawai* accumulates higher levels of  $\beta$ -carotene.** (a) and (b) show the levels of  $\beta$ -carotene and astaxanthin, respectively, in wild-type and lemon *T. kanzawai*. Carotenoid levels were determined by HPLC for both feeding and diapausing adult female mites. N.D. stands for not detected. Error bars represent the standard errors, with a sample size of three.



**Figure 4. Bulk segregant analysis locates the lemon locus and reveals a non-functional *CYP384A1* as the genetic basis.** (a) Differences in the frequencies of parental Jp-inbred-lemon alleles between each of the three lemon selected and one wild-type offspring pools are plotted in a sliding window analysis. The three *T. urticae* reference chromosomes are shown in alternating white and grey and are ordered by decreasing length. Dashed lines represent the 5% FDR for an association between parental Jp-inbred-lemon allele frequencies and the lemon phenotype. The maximal average allele frequency of the three replicates (i.e., the BSA peak) is located at cumulative genomic position 14,287,500. (b) *CYP384A1* and a 3' end fragment of its neighboring gene reside in the minimal candidate region. Gene models and their genomic position are based on the *T. urticae* genome annotation, with exons and introns depicted as dark and light grey rectangles, respectively. Strands are represented as "+" (forward) and "-" (reverse). Blue triangles delineate the genomic position of the genetic markers used in the fine-mapping approach and the vertical dotted lines demarcate the 8.96 kb minimal candidate region. The green triangle highlights the location of the BSA peak. (c) Read coverage reveals a deletion within the *CYP384A1* coding sequence in the three lemon selected offspring pools and parental Jp-inbred-lemon (black arrow). DNA sequence read coverage depth across the minimal candidate region is shown relative to the chromosome-wide average. (d) The deletion spans 246 bp within the fourth exon of the *CYP384A1* coding sequence concomitant with 7 bp of inserted sequence. The five essential cytochrome P450 domains are plotted above the gene models.

**Figure 5. *CYP384A1* is orthologous across mite species of the Trombidiformes order.** The maximum-likelihood phylogenetic reconstruction uncovered a 1:1:1:1 orthology of *CYP384A1* for the four trombidiform mite species with available genomic resources (Arthropoda: Chelicerata: Acari: Acariformes: Trombidiformes) (supplementary figure 5). The gene IDs for the identified orthologues are given in red font below the species name. A monophyletic origin for mites (Chelicerata: Acari) remains under debate [70].



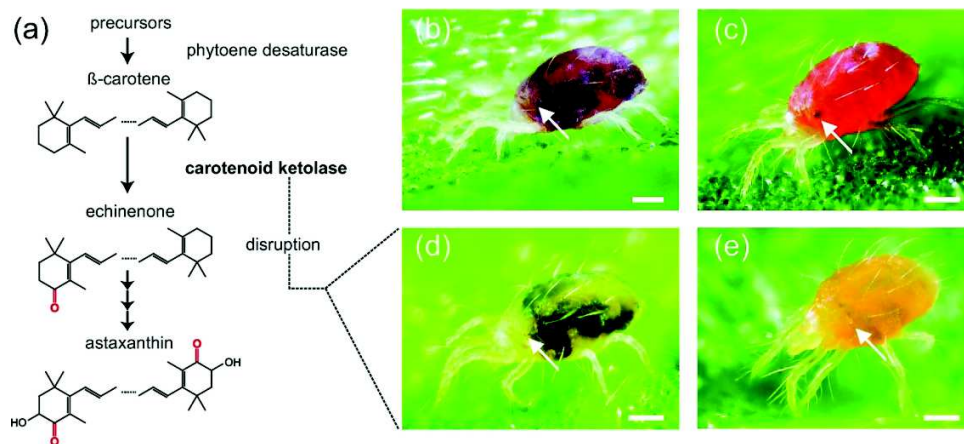


Figure 1. The conserved keto-carotenoid biosynthesis pathway in tetranychid mites and its disruption in lemon mutants. (a) The proposed pathway for carotenoid biosynthesis in spider mites [18] adapted to incorporate recent findings (endogenous synthesis of  $\beta$ -carotene by phytoene desaturase [4]).  $\beta$ -carotene is converted to echinenone, which leads to three major keto-carotenoids: 3-hydroxyechinenone and phoenicoxanthin (not shown), and astaxanthin [18]. Carotenoids are depicted in their de-esterified forms. (b) Wild-type *T. kanzawai*. (c) Wild-type diapausing *T. kanzawai*. (d) Lemon *T. kanzawai*. (e) Lemon diapausing *T. kanzawai*. Each panel depicts an adult female. Arrows highlight the anterior and posterior eye spots, which are red-colored in wild-type individuals. The dark regions in feeding, non-diapausing mites are gut contents that are visible through the partially translucent cuticle. Feeding spots are absent (or nearly so) in diapausing mites that have ceased to actively feed. Scalebars represent 0.1 mm.

138x64mm (300 x 300 DPI)

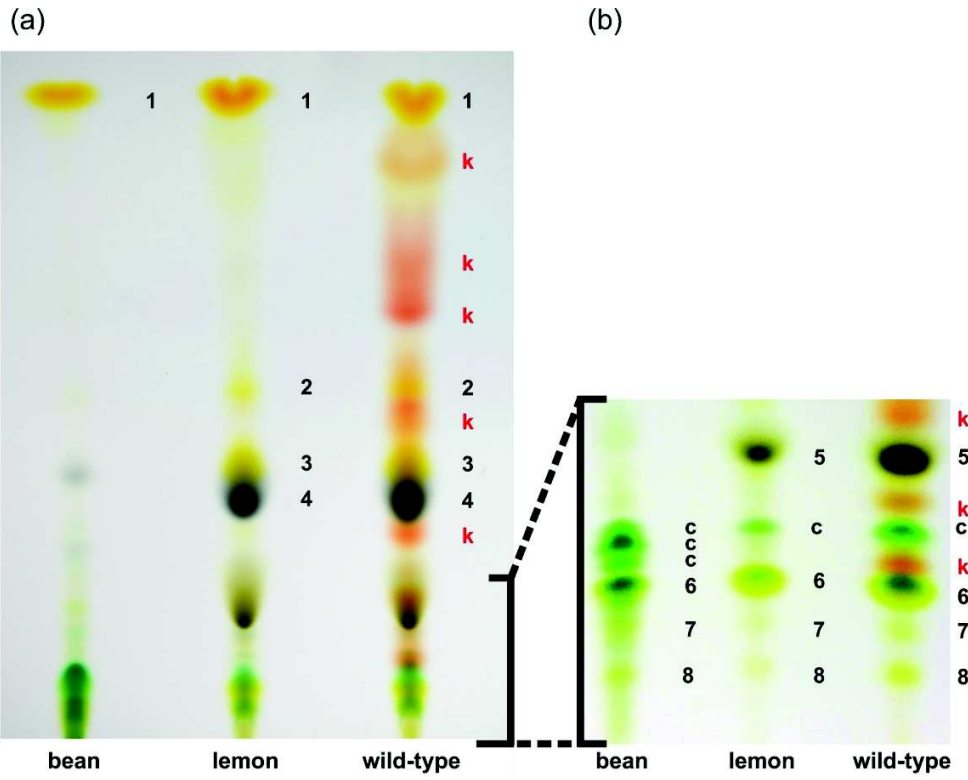


Figure 2. Lemon *T. kanzawai* lacks endogenously produced keto-carotenoids. (a) and (b) show HPTLC plates for plant and mite extracts run with mobile phases of 20% and 25% acetone in hexane, respectively. Using previously determined  $R_f$  values and color profiles [16–18], we tentatively identified the carotenoid pigments as: 1:  $\alpha$ - and  $\beta$ -carotene, k: keto-carotenoid (esterified in vivo), 2:  $\beta$ -carotene-diepoxide, 3: unknown epoxide, 4: chlorophyll a, 5: chlorophyll b, c: chlorophyll derivatives, 6: lutein and lutein 5,6-epoxide, 7: violaxanthin, and 8: neoxanthin.

143x120mm (300 x 300 DPI)

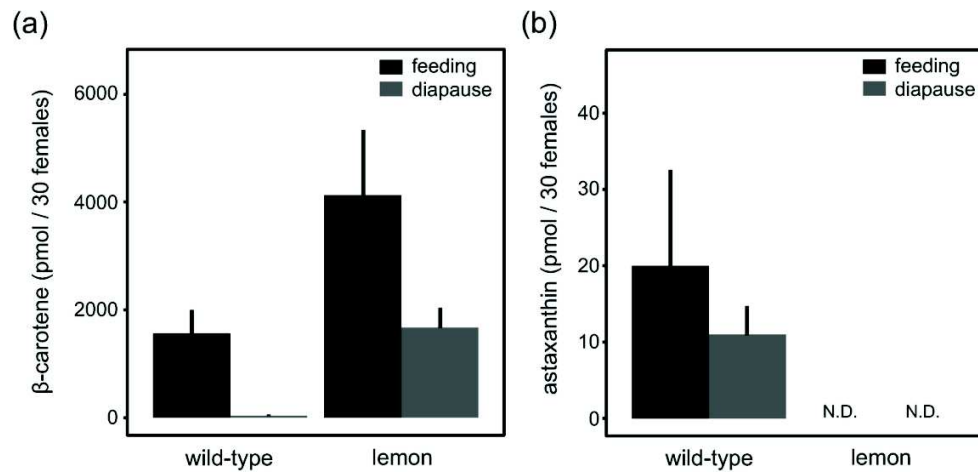


Figure 3. Lemon *T. kanzawai* accumulates higher levels of  $\beta$ -carotene. (a) and (b) show the levels of  $\beta$ -carotene and astaxanthin, respectively, in wild-type and lemon *T. kanzawai*. Carotenoid levels were determined by HPLC for both feeding and diapausing adult female mites. N.D. stands for not detected. Error bars represent the standard errors, with a sample size of three.

138x65mm (300 x 300 DPI)

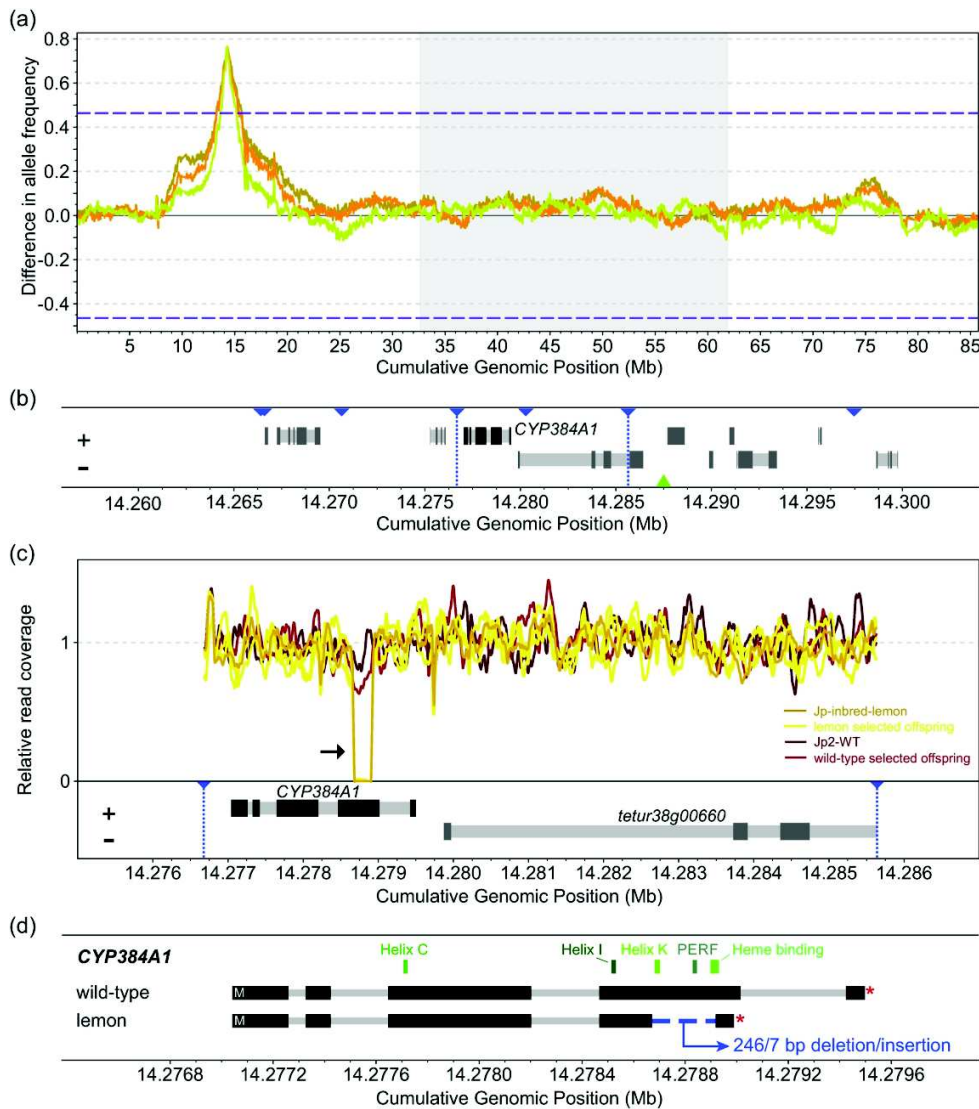


Figure 4. Bulked segregant analysis locates the lemon locus and reveals a non-functional CYP384A1 as the genetic basis. (a) Differences in the frequencies of parental Jp-inbred-lemon alleles between each of the three lemon selected and one wild-type offspring pools are plotted in a sliding window analysis. The three *T. urticae* reference chromosomes are shown in alternating white and grey and are ordered by decreasing length. Dashed lines represent the 5% FDR for an association between parental Jp-inbred-lemon allele frequencies and the lemon phenotype. The maximal average allele frequency of the three replicates (i.e., the BSA peak) is located at cumulative genomic position 14,287,500. (b) CYP384A1 and a 3' end fragment of its neighboring gene reside in the minimal candidate region. Gene models and their genomic position are based on the *T. urticae* genome annotation, with exons and introns depicted as dark and light grey rectangles, respectively. Strands are represented as "+" (forward) and "-" (reverse). Blue triangles delineate the genomic position of the genetic markers used in the fine-mapping approach and the vertical dotted lines demarcate the 8.96 kb minimal candidate region. The green triangle highlights the location of the BSA peak. (c) Read coverage reveals a deletion within the CYP384A1 coding sequence in the three lemon selected offspring pools and parental Jp-inbred-lemon (black arrow). DNA sequence read coverage depth across the minimal candidate region is shown relative to the chromosome-wide average. (d) The deletion spans 246 bp within the fourth exon of the CYP384A1 coding sequence concomitant with 7 bp of inserted sequence. The

five essential cytochrome P450 domains are plotted above the gene models.

184x209mm (300 x 300 DPI)

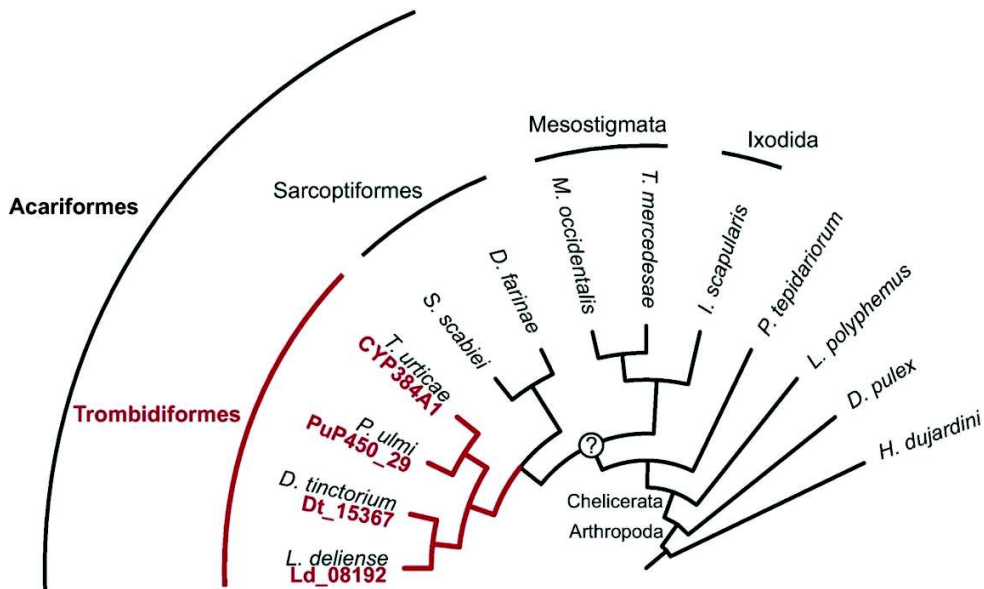


Figure 5. CYP384A1 is orthologous across mite species of the Trombidiformes order. The maximum-likelihood phylogenetic reconstruction uncovered a 1:1:1:1 orthology of CYP384A1 for the four trombidiform mite species with available genomic resources (Arthropoda: Chelicerata: Acari: Acariformes: Trombidiformes) (supplementary figure 5). The gene IDs for the identified orthologues are given in red font below the species name. A monophyletic origin for mites (Chelicerata: Acari) remains under debate [70].

107x64mm (300 x 300 DPI)



**Table 1. Lemon pigmentation has a recessive, monogenic mode of inheritance in *T. kanzawai***

Cross (♀ x ♂)	% lemon in F1 ♀ (2n)	F2 ♂ (n)		$\chi^2$	<i>p</i> -value
		wild-type	lemon		
Jp-WT x Jp-lemon	0	175	196	1.1887	0.2756
Jp-lemon x Jp-WT	0	365	372	0.066486	0.7965
Jp2-WT x Jp-lemon	0	198	210	0.35294	0.5525
Jp-lemon x Jp2-WT	0	187	174	0.46814	0.4938

The degrees of freedom for the  $\chi^2$ -tests were 1. For every cross, at least 70 F1 females were scored.